BIOMOLECULES & THERAPEUTICS

Original Article
Biomol Ther 30(6), 510-519 (2022)

Effects of Dextran Sulfate Sodium-Induced Ulcerative Colitis on the Disposition of Tofacitinib in Rats

Sung Hun Bae, Hyo Sung Kim, Hyeon Gyeom Choi, Sun-Young Chang and So Hee Kim*

College of Pharmacy and Research Institute of Pharmaceutical Science and Technology, Ajou University, Suwon 16499, Republic of Korea

Abstract

Tofacitinib, a Janus kinase 1 and 3 inhibitor, is mainly metabolized by CYP3A1/2 and CYP2C11 in the liver. The drug has been approved for the chronic treatment of severe ulcerative colitis, a chronic inflammatory bowel disease. This study investigated the pharmacokinetics of tofacitinib in rats with dextran sulfate sodium (DSS)-induced ulcerative colitis. After 1-min of intravenous infusion of tofacitinib (10 mg/kg), the area under the plasma concentration-time curves from time zero to time infinity (AUC) of tofacitinib significantly increased by 92.3%. The time-averaged total body clearance decreased significantly by 47.7% in DSS rats compared with control rats. After the oral administration of tofacitinib (20 mg/kg), the AUC increased by 85.5% in DSS rats. These results could be due to decreased intrinsic clearance of the drug caused by the reduction of CYP3A1/2 and CYP2C11 in the liver and intestine of DSS rats. In conclusion, ulcerative colitis inhibited CYP3A1/2 and CYP2C11 in the liver and intestines of DSS rats and slowed the metabolism of tofacitinib, resulting in increased plasma concentrations of tofacitinib in DSS rats.

Key Words: Tofacitinib, Ulcerative colitis, Dextran sulfate sodium, Pharmacokinetics, CYP3A1/2, CYP2C11

INTRODUCTION

Tofacitinib (Fig. 1) is a Janus kinase (JAK) 1 and 3 inhibitor developed for the treatment of rheumatoid arthritis (Claxton *et al*., 2018; Sandborn *et al*., 2022). The drug suppresses interleukins 2, 4, 7, 9, 15, and 21, which play essential roles in lymphocyte activation, proliferation, and functioning (Changelian *et al*., 2008; Flanagan *et al*., 2010). Tofacitinib was approved as the first oral JAK inhibitor for patients with moderate-to-severe ulcerative colitis who were not responsive to methotrexate (Fukuda *et al*., 2019). The half-life of tofacitinib is approximately 3.2 h and the absolute oral bioavailability (*F*) is approximately 74% when tofacitinib (10 mg) is orally administered to healthy volunteers (Cada *et al*., 2013; Scott, 2013; Dowty *et al*., 2014). In addition, approximately 70% of tofacitinib is metabolized by oxidation and *N*-demethylation by hepatic cytochrome P450 (CYP) 3A4 and CYP2C19, while 30% is excreted by the kidneys in an unmetabolized form (Dowty *et al*., 2014).

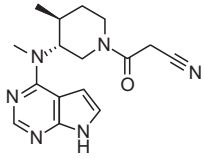

Fig. 1. Chemical structure of tofacitinib.

After the oral administration of tofacitinib (20 mg/kg) in male Sprague–Dawley rats, the *F* of tofacitinib was 29.1% and the amount remaining in the gastrointestinal tract at 24 h was 3.16% (Lee and Kim, 2019). The urinary excretion of tofacitinib was 10.0% of the 20 mg/kg dose administered orally to rats (Lee and Kim, 2019). In addition, the hepatic first-pass effect of tofacitinib is approximately 42.0% of the drug entering the portal vein and the intestinal first-pass effect is 46.1% of the intraduodenally administered dose (Lee and Kim, 2019). Therefore, systemic diseases that affect the function of the liver, intestine, or kidney could change the pharmacokinetics of tofacitinib owing to a significant first-pass effect of tofacitinib in the liver and intestines. In a streptozotocin-induced diabetes mellitus rat model, the protein expression of CYP3A1/2 in the intestine and liver increased, resulting in an increase in

Open Access **https://doi.org/10.4062/biomolther.2022.049**

Received Apr 14, 2022 **Revised** Jun 7, 2022 **Accepted** Jun 9, 2022
Published Online Jul 11, 2022

***Corresponding Author**
E-mail: shkim67@ajou.ac.kr
Tel: +82-31-219-3451, Fax: +82-31-219-3435

the intestinal and hepatic intrinsic clearance (CL_{int}) of tofacitinib and a decrease in the plasma concentration of tofacitinib (Gwak *et al*., 2020). The *F* value decreased with the increased expression of P-glycoprotein (P-gp) as well as faster CL_{int} in the intestine (Gwak *et al*., 2020). In a rat model of cisplatin-induced acute renal failure, renal excretion of tofacitinib was significantly reduced owing to the deterioration of renal function. Additionally, drug metabolism was also reduced due to a significant decrease in hepatic CYP3A1/2 after intravenous and oral administration of tofacitinib, which resulted in an increased plasma concentration of tofacitinib (Bae *et al*., 2020).

Ulcerative colitis and Crohn's disease are the representative chronic inflammatory bowel diseases (Ordas *et al*., 2012). There are various causes of ulcerative colitis; however, in general, a strong genetic predisposition, environmental factors (eating habits, smoking, etc.), changes in the intestinal microbiota due to infection, and abnormal regulation of the immune system are mentioned (Taurog *et al*., 1994; Baumgart and Carding, 2007; Sartor, 2008). In general, chronic inflammation increases lipopolysaccharides in the blood, which migrate to the liver, cause hepatic inflammation, and produce various inflammatory cytokines (Pastor Rojo *et al*., 2007), known to downregulate the expression and activity of CYP enzymes (Masubuchi and Horie, 2004; Chen *et al*., 2008). In patients with ulcerative colitis, the plasma concentration of cyclosporin increased by five times (Latteri *et al*., 2001) and that of metronidazole increased by 50% (Bergan *et al*., 1981). In addition, in a dextran sulfate sodium (DSS)-induced ulcerative colitis mouse model, mRNA and protein expression of hepatic CYP isoforms decreased and the CL_{int} of triazolam also decreased (Kusunoki *et al*., 2014). Based on the above reports, pharmacokinetic changes of a drug may be expected due to an increase in plasma concentration by decreasing drug metabolism in patients with ulcerative colitis.

Therefore, this study aimed to evaluate the pharmacokinetic changes of tofacitinib after it was administered intravenously and orally to DSS-induced ulcerative colitis rats and to validate the activity and protein expression of drug-metabolizing enzymes in the liver and intestine.

MATERIALS AND METHODS

Chemicals

Tofacitinib and hydrocortisone [an internal standard for high-performance liquid chromatography (HPLC) analysis] were purchased from Sigma-Aldrich (St. Louis, MO, USA). To induce ulcerative colitis in rats, DSS was obtained from MP Biomedicals (Illkirch, France) and β-cyclodextrin was obtained from Wako (Osaka, Japan). Heparin and 0.9% NaCl-injectable solutions were manufactured by the JW Pharmaceutical Corporation (Seoul, Korea). Primary antibodies against CYP1A1/2, CYP2B1/2, CYP2C11, CYP2D1, CYP2E1, and CYP3A1/2 were obtained from Detroit R&D Inc. (Detroit, MI, USA). Primary antibodies against pregnane X receptor (PXR), constitutive androstane receptor (CAR), P-gp and β-actin were purchased from Cell Signaling Technology (Beverly, MA, USA). Secondary goat, rabbit, and mouse antibodies were supplied by Bio-Rad (Hercules, CA, USA). All the other chemicals and reagents were of HPLC or analytical grade and were used as received without further purification.

Animals

Sprague–Dawley male rats (6 weeks old, weight 160-180 g) were obtained from OrientBio (Seongnam, Korea). They were individually managed in a clean room maintained at 21-23°C under 12 h (07:00-19:00) light and 12 h (19:00-07:00) dark cycles with 45-55% relative humidity through air purification (Laboratory Animal Research Center of Ajou University Medical Center, Suwon, Korea). Rats were treated according to previously published methods (Lee and Kim, 2019; Park *et al*., 2021). All the rats were provided free access to food and water without any restrictions. The animal experiments and protocols were reviewed based on standard operating procedures and were approved by the Institutional Animal Care and Use Committee (IACUC No. 2020-0013).

Induction of ulcerative colitis

The rats were randomly assigned to two experimental groups, control (CON) and dextran sulfate sodium-induced ulcerative colitis (DSS) rats. Ulcerative colitis was induced in the DSS group for 10 days by feeding the rats 5% DSS (w/v) dissolved in their drinking water, while CON rats received drinking water without added DSS (Hu *et al*., 2020). Both groups of rats had free access to food. The day after the last drinking of DSS water, plasma was obtained from CON and DSS rats (n=3 per group). All the rats were sacrificed by light anesthesia with ketamine (100 mg/kg). The entire colons were removed and the length of the colon was measured.

Preliminary study

The albumin, total protein, serum creatinine (S_{CR}), glutamate pyruvate transaminase (GPT) and glutamate oxaloacetate transaminase (GOT) levels were measured in the plasma samples of CON and DSS rats (Green Cross Reference Lab, Seoul, Korea). To estimate creatinine clearance (CL_{CR}), urine samples were collected for 24 h and urine volumes and creatinine levels were measured. CL_{CR} was estimated by dividing the amount of creatinine excreted in the urine over 24 h by the area under the plasma concentration-time curve of creatinine from 0 to 24 h ($AUC_{0\text{-}24\ h}$) (Bae *et al*., 2020). For tissue biopsies, whole kidneys and livers were removed from CON and DSS rats and weighed. A small portion of liver, kidney, and colon was excised and fixed in 10% neutral buffered formalin (BBC Biochemical, Mount Vernon, WA, USA).

Rat plasma protein binding of tofacitinib

Equilibrium dialysis (Kim *et al*., 1999) was performed to measure the plasma protein binding of tofacitinib using fresh plasma obtained from CON and DSS rats (n=3, each group). Briefly, 1 mL of plasma from CON or DSS rats was dialyzed against an equal volume of isotonic Sørensen phosphate buffer (pH 7.4) through a Spectra/Por 2 membrane (molecular weight cutoff 12,000-14,000 Da; Spectrum Medical Industries, Los Angeles, CA, USA). To minimize the time required to reach equilibrium, 10 μg/mL tofacitinib was spiked into the plasma compartment (Svein and Theodor, 1982; Shin *et al*., 1991). After incubation at 37°C in a water bath at 50 opm for 24 h, 50 μL was aliquoted from each compartment and the concentration of tofacitinib in the plasma (C_P) and buffer (C_B) compartments was analyzed using HPLC (Kim *et al*., 2020). Percent binding (%) was calculated as follows:

$$\text{Percent binding (\%)} = \frac{C_P - C_B}{C_P} \times 100$$

Intravenous and oral administration of tofacitinib

For the intravenous study, the jugular vein and carotid artery were cannulated using polyethylene tubing 50 (Clay Adams, Parsippany, NJ, USA) for drug administration and blood collection, respectively. For the oral study, the rats were fasted overnight and only the carotid artery was cannulated for blood collection. All surgical procedures were performed after anesthesia with ketamine (100 mg/kg) and experiments commenced after a sufficient recovery time of 3-4 h after anesthesia (Park *et al*., 2021).

For the intravenous study, tofacitinib (dissolved in 0.9% NaCl-injectable solution containing 0.5% β-cyclodextrin) was administered intravenously via the jugular veins of the CON (*n*=7) and DSS (*n*=6) rats at a dose of 10 mg/kg. Blood samples (0.12 mL) were obtained at 0 (prior to drug administration), 1, 5, 15, 30, 45, 60, 90, 120, 180, 240, and 360 min through the carotid artery. Tofacitinib (the same solution used in the intravenous study) was also administered orally to CON (*n*=6) and DSS (*n*=6) rats at a dose of 20 mg/kg. Blood samples (0.12 mL) were collected through the carotid artery at 0 (prior to drug administration), 5, 15, 30, 45, 60, 90, 120, 180, 240, 360, 480, 600, and 720 min. After collecting blood samples, 0.3 mL of heparinized 0.9% NaCl-injectable solution (10 IU/mL) was immediately flushed into the carotid artery to prevent blood clotting. Blood samples were centrifuged for 1 min at 8,000 *g* and plasma (50 μL) was collected (Kim *et al*., 2020).

At 24 h, the abdomen of each rat was opened and the entire gastrointestinal tract was collected, cut into small pieces, and immersed in a beaker containing 50 mL of methanol. After evenly mixing the contents of the beaker, 50 μL of the supernatant was collected (Kim *et al*., 2020). Urine samples were collected 24 h after drug administration. After measuring the urine volume, two 100 μL aliquots of each urine sample were collected (Kim *et al*., 2020). All samples were stored at –80°C in a deep freezer until HPLC analysis for tofacitinib was performed (Kim *et al*., 2020).

Tissue distribution of tofacitinib

Rats were treated according to previously published methods (Lee and Kim, 2019; Park *et al*., 2021). Approximately 30 min after the intravenous administration of tofacitinib (10 mg/kg) to CON and DSS rats (*n*=3 in each group), maximum possible volume of blood was collected from the carotid artery and immediately centrifuged to obtain plasma. Fat, brain, kidney, heart, liver, large intestine, mesentery, lung, small intestine, muscle, stomach, and spleen were removed and rinsed in phosphate buffer solution (pH 7.4) to remove the remaining blood. Approximately 1 g of each tissue was added to four volumes of homogenizing buffer, homogenized (T25 Ultra-Turrax, IKA Labortechnik, Staufen, Germany), and centrifuged at 8,000 *g* for 10 min. An aliquot (50 μL) of the supernatant was collected and stored at –80°C until HPLC analysis of tofacitinib was performed (Kim *et al*., 2020).

Measurement of V_{max}, K_m, and CL_{int}

The experiments were conducted as previously reported (Bae *et al*., 2020; Gwak *et al*., 2020) for the preparation of hepatic and intestinal microsomes. Protein concentrations of hepatic and intestinal microsomes were estimated using the bicinchoninic acid method. Microsomes (1 mg/mL protein content), 1 μL of various concentrations of tofacitinib (0.5, 0.75, 1, 2, 5, 10, and 20 μM) and a nicotinamide adenine dinucleotide phosphate hydrogen-generating system (Corning Inc., Corning, NY, USA) were combined to simulate an *in vivo* metabolic system. The total volume of the system was adjusted to 1 mL by adding 0.1 M phosphate buffer (pH 7.4). The contents were incubated at 50 oscillations per min (opm) in a 37°C water bath for 15 min and the reaction was terminated by adding twice the volume of methanol. Kinetic constants, maximum velocity (V_{max}) and apparent Michaelis–Menten constant (K_m; the concentration at which the rate is one-half of V_{max} for the metabolism of tofacitinib) were measured using a Lineweaver–Burk plot followed by nonlinear regression analysis (Duggleby, 1995; Gwak *et al*., 2020) using Prism 5 (GraphPad Software Inc., San Diego, CA, USA). The CL_{int} for tofacitinib metabolism was calculated by dividing V_{max} by K_m (Duggleby, 1995; Gwak *et al*., 2020).

Immunoblot analysis

Hepatic and intestinal microsomes (20-40 μg protein per lane) were resolved by 10% sodium dodecyl sulfate polyacrylamide gel electrophoresis and transferred to a nitrocellulose membrane for 1 h. For immunodetection, blots were incubated on a shaker overnight with primary antibodies against CYP1A1/2, CYP2B1/2, CYP2C11, CYP2D1, CYP2E1, CYP3A1/2, P-gp, PXR, or CAR diluted in Tris-buffered saline with 0.1% Tween 20 (TBS-T) containing 5% bovine serum albumin (1:2,000) at 4°C. The blots were then incubated with a horseradish peroxide-conjugated secondary antibody diluted 1:10,000 in TBS-T containing 5% skim milk for 1 h at room temperature. Protein expression was visualized by enhanced chemiluminescence (Bio-Rad) using an Image Quant LAS 4000 Mini (GE Healthcare Life Sciences, Piscataway, NJ, USA) and band density was measured using ImageJ 1.45s software (NIH, Bethesda, MA, USA). β-Actin was used as an internal standard (Bae *et al*., 2020).

HPLC analysis

Analysis of tofacitinib concentration in biological samples was performed using previously published method (Kim *et al*., 2020). Briefly, 50 μL of biological sample was mixed with 1 μL of hydrocortisone (an internal standard, 5 mg/mL) and then 20% ammonia solution (20 μL) was added. The mixture was vortexed for 30 s and extracted with 750 μL of ethyl acetate. The organic layer was collected and evaporated under a gentle flow of nitrogen gas at 40°C (Eyela, Tokyo, Japan). The residue was then redissolved in 130 μL of 20% acetonitrile and 50 μL of the supernatant was analyzed using a reversed-phase column (C_{18}; 250×4.6 mm, 5 μm; Young Jin Biochrom, Seongnam, Korea).

The concentration of tofacitinib in the biological samples was determined using a Prominence LC-20A HPLC system (Shimadzu, Kyoto, Japan). The mobile phase consisted of 10 mM ammonium acetate buffer (pH 5.0) and acetonitrile in a 69.5:30.5 (v/v) ratio with a flow rate of 1 mL/min. Measurements were performed using a UV detector set at 287 nm. The retention times of tofacitinib and hydrocortisone were approximately 7.21 and 11.3 min, respectively. The lower limits of quantitation of tofacitinib in rat plasma and urine were 0.01

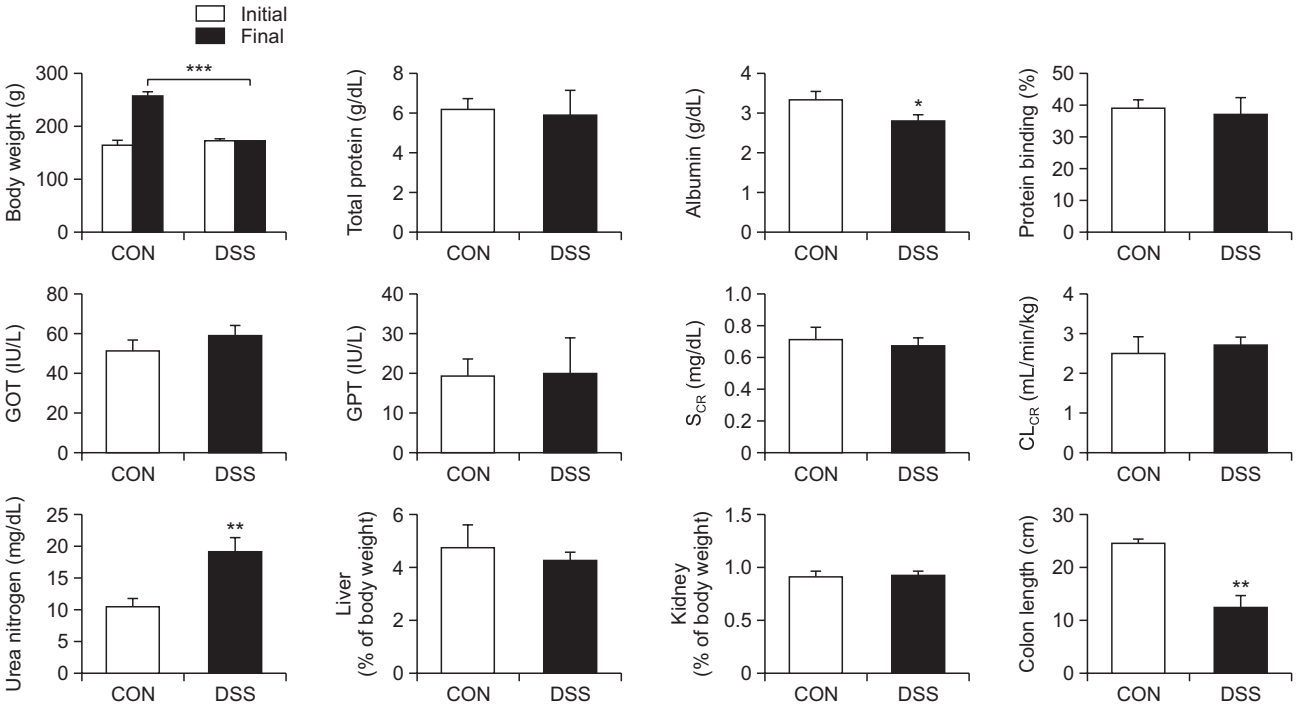

Fig. 2. Body weight, plasma chemistry data, creatinine clearance (CL_{CR}), plasma protein binding of tofacitinib, relative liver and kidney weights, and colon length in control (CON) and dextran sulfate sodium-induced ulcerative colitis (DSS) rats. Data are shown as mean ± standard deviation (n=3, each group). GOT, glutamate oxaloacetate transaminase; GPT, glutamate pyruvate transaminase; S_{CR}, serum creatinine concentration. *p<0.05, **p<0.01 and ***p<0.001.

and 0.1 μg/mL, respectively. The intraday assay precisions (coefficients of variation, CVs) in rat plasma and urine were 3.69%-5.88% and 4.21%-6.18%, respectively and the corresponding inter-day assay precisions were 5.06% and 5.46%, respectively (Kim *et al*., 2020).

Pharmacokinetic analysis

The following pharmacokinetic parameters were determined by non-compartmental analysis (WinNonlin, Pharsight Corporation, Mountain View, CA, USA) using standard methods (Gibaldi and Perrier, 1982): terminal half-life, time-averaged total body clearance (CL), renal clearance (CL_R), nonrenal clearance (CL_{NR}), apparent volume of distribution at steady state (V_{ss}), and AUC. The AUC values were calculated using the trapezoidal rule–extrapolation method (Chiou, 1978), while peak plasma concentration (C_{max}) and time to reach C_{max} (T_{max}) were obtained directly from the plasma concentration-time profiles.

Statistical analysis

All experimental results are presented as mean ± standard deviation (SD) and only T_{max} is expressed as a median (range) value. Comparisons between the two groups were performed using an unpaired Student's *t*-test. A p value <0.05 was determined statistically significant.

RESULTS

Induction of ulcerative colitis

Ulcerative colitis was induced by drinking 5% DSS (w/v) dissolved in water. Surrogate symptoms of ulcerative colitis, such as diarrhea and bloody excrement, were observed in DSS rats. Body weight gain was not observed in DSS rats (1.14% decrease) compared to CON rats (52.4% increase). In addition, a significant decrease in colon length (49.0% decrease) was also found in DSS rats compared to CON rats (Fig. 2, 3A). Considerable tissue alterations were observed in the colon microscopy of DSS rats, including loss of crypt, edema with thickened tissue, and inflammation (Fig. 3B).

Plasma concentrations of total protein, GOT, GPT, and S_{CR} were similar and were not significantly different between CON and DSS rats (Fig. 2). However, albumin was significantly decreased by 15.8% and urea nitrogen was significantly increased by 86.4% in DSS rats (Fig. 2). The relative weights (% of body weight) of the liver and kidney did not significantly differ and there were no histological changes in the liver and kidney between CON and DSS rats (Fig. 2, 3B).

Plasma protein binding of tofacitinib

The plasma protein binding of tofacitinib to 4% human serum albumin, similar to the ratio in rat plasma (Mitruka and Rawnsley, 1981), was independent of tofacitinib concentrations, ranging from 1 to 100 μg/mL (Kim *et al*., 2020). Therefore, 10 μg/mL tofacitinib was chosen for the plasma protein-binding study. The protein binding values of tofacitinib to fresh plasma from CON and DSS rats were 39.4 ± 2.17% and 37.4 ± 4.71%, respectively (Fig. 2). There were no significant differences between the two groups of rats.

Intravenous administration study

Fig. 4A shows the mean arterial plasma concentration ver-

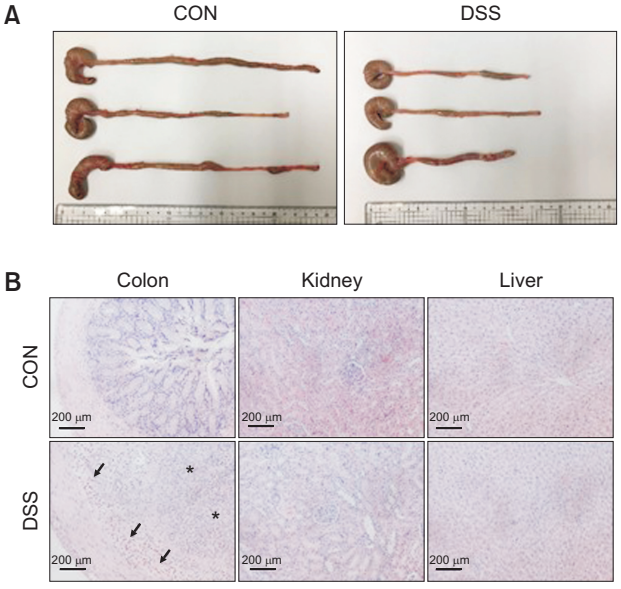

Fig. 3. (A) Macroscopic changes in the colons of control (CON) and dextran sulfate sodium-induced ulcerative colitis (DSS) rats. (B) Colon, kidney and liver biopsies in CON and DSS rats. Black arrow indicates the infiltration of polymorphonuclear cells such as neutrophils and star(*) represents crypt loss filled with infiltration of immune cells.

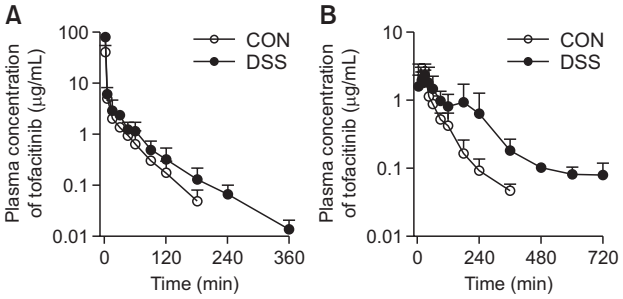

Fig. 4. Mean arterial plasma concentration-time profiles of tofacitinib after (A) 1-min intravenous infusion (10 mg/kg) to control (CON, open, *n*=7) and dextran sulfate sodium-induced ulcerative colitis (DSS, closed, *n*=6) rats and (B) oral administration (20 mg/kg) to CON (open, *n*=6) and DSS (closed, *n*=6) rats. Each bar represents the standard deviation.

sus time curves of tofacitinib following a 1-min intravenous infusion of tofacitinib at a dose of 10 mg/kg to CON (*n*=7) and DSS (*n*=6) rats. The relevant pharmacokinetic parameters are listed in Table 1. The plasma concentration of tofacitinib declined polyexponentially, with terminal half-lives of 31.0 and 42.0 min in CON and DSS rats, respectively. The plasma concentration of tofacitinib in DSS rats was higher than that in CON rats and the AUC of tofacitinib in DSS rats was significantly greater (92.3% increase) than that in CON rats. The greater AUC of tofacitinib was presumed to be due to the slower CL (47.7% decrease) in DSS rats. This result supported the slowing down of tofacitinib metabolism by slower CL_{NR} (45.3% decrease) in DSS rats than in CON rats. The CL_R of tofacitinib was also significantly slower (77.6% decrease) in DSS rats that in CON rats (Table 1). Furthermore, the V_{ss} value was significantly lower by 43.2% in DSS rats than in CON rats. However, the remaining percentages of tofacitinib in the gastrointestinal tract 24 h after drug administration ($GI_{24\ h}$) were low, 0.484% and 0.328% of the intravenous dose in CON and DSS rats, respectively, with no significant differences between the two groups.

Oral administration study

Fig. 4B shows the mean arterial plasma concentration versus time curves of tofacitinib following oral administration at a dose of 20 mg/kg to CON (*n*=6) and DSS (*n*=6) rats. The relevant pharmacokinetic parameters are summarized in Table 1. Tofacitinib was absorbed rapidly in the gastrointestinal tract and detected at the first blood collection time (5 min) in all the rats. The plasma concentrations of tofacitinib in DSS rats were higher than those in CON rats, with the AUC value significantly greater by 85.5% in DSS rats than in CON rats. Owing to the relatively greater AUC values in DSS rats, the CL_R values were significantly lower by 64.0% in DSS rats than in CON rats. Even though $GI_{24\ h}$ of orally administered tofacitinib was significantly greater in DSS rats (1.10%) than in CON rats (0.124%), the values were relatively low, indicating that the absorption of tofacitinib from the gastrointestinal tract was almost complete in both groups. The *F* values of tofacitinib after oral administration were 29.3% and 28.3% in CON and DSS rats, respectively.

Tissue distribution of tofacitinib

The tissue concentration (μg/mL for plasma and μg/g for tissue) and tissue-to-plasma (T/P) ratio at 30 min after intravenous administration of 10 mg/kg tofacitinib are shown in Fig. 5. Tofacitinib was widely distributed in rat tissues of both groups. However, the plasma concentration of tofacitinib was significantly higher in DSS group than that in CON group. The concentrations of tofacitinib in the stomach, small intestine, and mesentery of DSS rats were significantly higher than those of CON rats, whereas the concentrations of tofacitinib in other tissues were not significantly different between the two groups (Fig. 5A). Although the T/P ratios were not statistically significant, the ratios (except for mesentery) in DSS rats showed a generally lower or similar trend compared to CON rats due to the higher plasma concentration of tofacitinib in DSS rats (Fig. 5B).

In vitro metabolism of tofacitinib

To confirm the *in vitro* metabolism of tofacitinib, V_{max}, K_m, and CL_{int} values in the hepatic and intestinal microsomes of CON and DSS rats are shown in Fig. 6. The V_{max} value in the hepatic microsomes of DSS rats significantly decreased to 15.4% of that in CON rats. The K_m value in hepatic microsomes was comparable between CON and DSS rats. Therefore, the CL_{int} for the disappearance of tofacitinib in hepatic microsomes was significantly decreased by 75.5% in DSS rats compared with CON rats (Fig. 6A).

In context of intestinal microsomes, the V_{max} and K_m values of tofacitinib were comparable in both CON and DSS rats (Fig. 6B). However, the CL_{int} decreased by 39.1% in DSS rats compared with that in CON rats (5.81 vs. 3.54 μL/min/mg protein, *p*=0.0679). These results suggest that the metabolism of tofacitinib in the rat liver and intestine is affected by DSS-induced ulcerative colitis.

Table 1. Pharmacokinetic parameters of tofacitinib after 1-min intravenous infusion at a dose of 10 mg/kg and oral administration at a dose of 20 mg/kg to control (CON) and dextran sulfate sodium-induced ulcerative colitis (DSS) rats

	Intravenous		Oral	
	CON (*n*=7)	DSS (*n*=6)	CON (*n*=6)	DSS (*n*=6)
Body weight (g)	297 ± 47.3	225 ± 17.4*	256 ± 10.7	187 ± 23.9***
AUC (μg·min/mL)	271 ± 42.9	521 ± 58.4***	159 ± 19.8	295 ± 53.7***
C_{max} (μg/mL)			2.36 ± 0.587	2.46 ± 1.05
T_{max} (min)			19.2 ± 12.4	25.0 ± 15.4
Terminal half-life (min)	31.0 ± 5.36	42.0 ± 11.8*		
MRT (min)	20.3 ± 7.24	31.9 ± 25.5		
CL (mL/min/kg)	37.1 ± 5.68	19.4 ± 2.26***		
CL_R (mL/min/kg)	3.07 ± 1.40	0.688 ± 0.149**	5.47 ± 4.05	1.97 ± 1.14*
CL_{NR} (mL/min/kg)	34.0 ± 5.54	18.6 ± 1.65***		
V_{ss} (mL/kg)	767 ± 286	436 ± 164*		
$Ae_{0\text{-}24\ h}$ (% of dose)	3.97 ± 2.93	2.73 ± 1.89	4.13 ± 2.71	2.40 ± 1.26
$GI_{24\ h}$ (% of dose)	0.484 ± 0.298	0.328 ± 0.438	0.124 ± 0.141	1.10 ± 0.782*
F (%)			29.3	28.3

Data are shown as mean ± standard deviation.

$Ae_{0\text{-}24\ h}$, the drug excreted as an unchanged form in the urine for 24 h; AUC, area under plasma concentration-time curves from time zero to time infinity; C_{max}, maximum plasma concentration; CL, time-averaged total body clearance; CL_{NR}, time-averaged non-renal clearance; CL_R, time-averaged renal clearance; *F*, absolute oral bioavailability; $GI_{24\ h}$, the percentage of drug remaining in the gastrointestinal tract at 24 h; MRT, mean residence time; T_{max}, time to reach C_{max}; V_{ss}, the apparent volume of distribution at steady state. *p<0.05, **p<0.01, ***p<0.001.

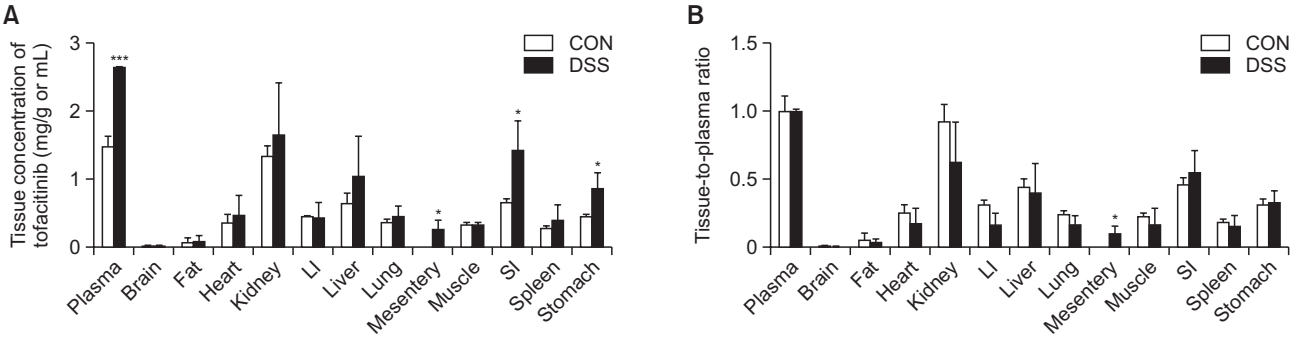

Fig. 5. (A) Mean tissue concentration (μg/mL plasma or μg/g tissue) and (B) the tissue concentration-to-plasma concentration (T/P) ratios of tofacitinib 30 min after a 1-min intravenous infusion of 10 mg/kg to control (CON, white) and dextran sulfate sodium-induced ulcerative colitis (DSS, black) rats (*n*=3, each group). Data are shown as mean ± standard deviation. LI, large intestine; SI, small intestine. *p<0.05 and ***p<0.001.

Effect of ulcerative colitis on the expression of CYP and other related proteins

The protein expression of hepatic and intestinal CYP isozymes, nuclear receptors (PXR and CAR), and P-gp in CON and DSS rats is shown in Fig. 7. The protein expression of CYP1A1/2, CYP2B1/2, CYP2C11, CYP3A1/2, and CYP2E1 was remarkably decreased in the hepatic microsomes of DSS rats, whereas CYP2D6 was comparable between CON and DSS rats (Fig. 7A). Similarly, the protein expression of CYP1A1/2, CYP2B1/2, CYP2C11, CYP3A1/2, and CYP2E1, including CYP2D6, also decreased in the intestinal microsomes of DSS rats (Fig. 7A). These findings suggest that DSS-induced ulcerative colitis affected the protein expression of CYP isozymes and might result in changes in the metabolism of tofacitinib. Furthermore, the protein expression of PXR and CAR, transcriptional regulators of CYP3A and CYP2C subfamily (Wada *et al*., 2009; Daujat-Chavanieu and Gerbal-Chaloin, 2020) and P-gp was also decreased in the liver and intestine of DSS rats (Fig. 7B).

DISCUSSION

DSS has been widely used to establish an ulcerative colitis model in mice and rats because pathological and etiological conditions as well as therapeutic reactions are similar to the active stage of ulcerative colitis in humans (Solomon *et al*., 2010). DSS accumulates in the lamina propria mucosae of the colon, and is phagocytized by macrophages, thereby initiating inflammation (Okayasu *et al*., 1990). Typical symptoms, such as body weight loss and bloody diarrhea, were observed in rats with DSS-induced ulcerative colitis (Kusunoki *et al*., 2014) as well as shortened colon lengths. The colon biopsies in this study also demonstrated the induction of severe ulcerative colitis in rats, showing crypt loss filled with infiltration of immune cells, edema with thickened tissue, and infiltration of

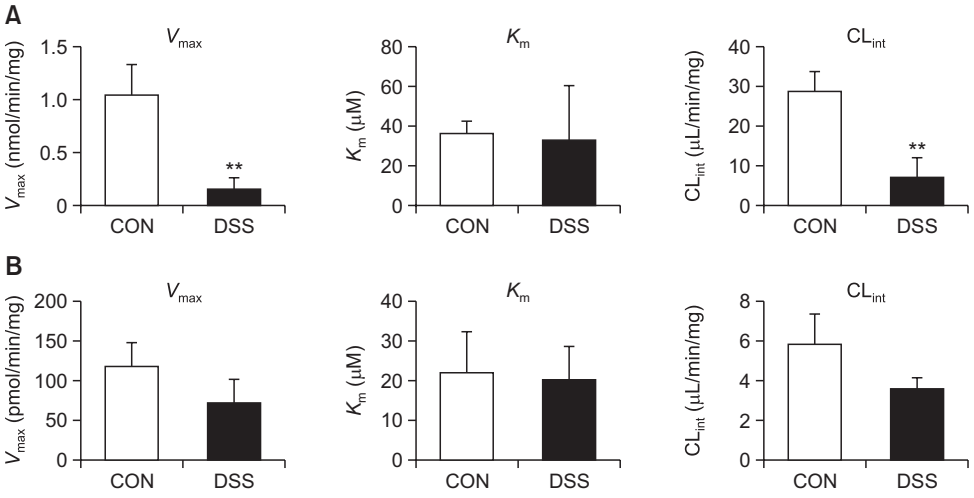

Fig. 6. Mean values of V_{max}, K_m and CL_{int} for the disappearance of tofacitinib in (A) hepatic and (B) intestinal microsomes from control (CON, white) and dextran sulfate sodium-induced ulcerative colitis (DSS, black) rats (n=3 per group). This experiment was completed three times. Data are shown as mean ± standard deviation. V_{max}, maximum velocity; K_m, apparent Michaelis–Menten constant; CL_{int}, intrinsic clearance. **p<0.01.

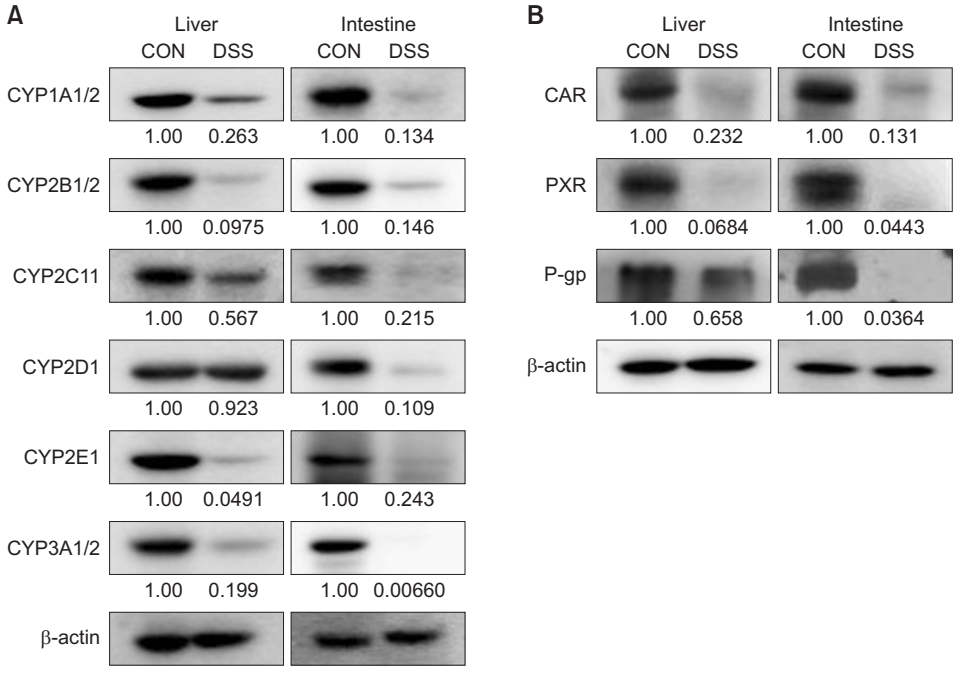

Fig. 7. Immunoblot analyses of (A) CYP450 isozymes and (B) PXR, CAR and P-gp of hepatic and intestinal microsomes in control (CON) and dextran sulfate sodium-induced ulcerative colitis (DSS) rats. β-actin was determined as a loading control. This experiment was completed three times. Band density was measured using ImageJ1.45s software (NIH). CAR, constitutive androstane receptor; PXR, pregnane X receptor; P-gp, P-glycoprotein.

polymorphonuclear cells, such as neutrophils (Fig. 3B).

The gastrointestinal and biliary excretion of tofacitinib represented by $GI_{24\ h}$ was insignificant (less than 0.484% of the intravenous dose) in both CON and DSS rats, indicating that the contribution of gastrointestinal and biliary excretion of tofacitinib to CL_{NR} could be negligible. This lower $GI_{24\ h}$ was presumably not due to chemical or enzymatic degradation of tofacitinib in the gastrointestinal tract of rats because tofacitinib is stable in various pH buffers (pH 2-10) and rat gastric juice (pH 3.5) for 24 h (Kim *et al*., 2020). Additionally, 0.703% of intravenous tofacitinib (10 mg/kg) in rats (n=3) was excreted in the bile for 24 h as unchanged tofacitinib (Lee and Kim, 2019). These results indicated that the CL_{NR} values in Table 1 represent metabolic elimination as the contribution of $GI_{24\ h}$ to CL_{NR} was marginal.

After intravenous administration of tofacitinib, the signifi-

cantly greater AUC of tofacitinib appeared to be due to the significantly slower CL in DSS rats than in CON rats (Table 1). The slower CL in DSS rats was mainly due to the significantly slower CL_{NR} compared to that in CON rats. The CL_R of tofacitinib was also significantly slower in DSS rats than that in CON rats, but its contribution to CL of tofacitinib seemed to be minimal (8.27% and 3.55% for CON and DSS rats, respectively; Table 1). Thus, the contribution of CL_R to other pharmacokinetic parameters appeared to be minor. The slower CL_{NR} of tofacitinib in DSS rats was supported by the significantly slower *in vitro* hepatic CL_{int} (Fig. 6A) and slower hepatic blood flow (Mori *et al*., 2005) in DSS rats compared to those in CON rats. In the ulcerative colitis disease model, the intestinal blood flow was reduced (Mori *et al*., 2005) and the blood flow from intestine supplied to the liver through the portal vein (Liu *et al*., 2021). Therefore, it was presumed that the intestinal-associated hepatic blood flow would decrease in the DSS rats. The plasma protein binding of tofacitinib did not affect CL_{NR} of tofacitinib by DSS-induced ulcerative colitis, because the plasma protein binding of tofacitinib was not high (37.4%-39.4%); thus, the free fractions of tofacitinib were comparable between CON and DSS rats (Fig. 2).

Tofacitinib is a drug with an intermediate hepatic extraction ratio (30%-70%) because the hepatic first-pass metabolism after absorption into the portal vein was 42.0% in rats (Lee and Kim, 2019). The slower hepatic CL_{int} in DSS rats was supported by a decrease in the protein expression of CYP3A1/2 and CYP2C11 by 80.1% and 43.3%, respectively. Similar results were reported in a DSS mouse model, where the plasma concentration of omeprazole was increased due to the decreased hepatic expression of CYP1A2, CYP2D1, and CYP3A1 (Hu *et al*., 2020). The decreased expression of hepatic CYP3A1/2 and CYP2C11 was due to a decrease in the expression of PXR and CAR, the transcription factors of CYP isoforms, in the liver of DSS-induced ulcerative colitis mice (Kusunoki *et al*., 2014; Fan *et al*., 2020). Furthermore, lipopolysaccharide-induced ulcerative colitis causes hepatic inflammation by combining with toll-like receptor 4 in the hepatic Kupffer cells of DSS-induced ulcerative colitis mice, secretes cytokines such as interleukin 6, and increases nuclear factor-κB activity (Kusunoki *et al*., 2014). This reduces PXR and CAR transcription, which decreases the activity and expression of CYP3A and CYP2C subfamilies in a DSS-induced ulcerative colitis mouse model (Kusunoki *et al*., 2014).

Following the intravenous administration of tofacitinib, CL_R was recalculated (CL_R') from the free (unbound to plasma proteins) fractions of the drug in plasma based on CL_R (Table 1) and the plasma protein binding values of tofacitinib (Fig. 2); CL_R' values were estimated to be 5.07 and 1.10 mL/min/kg for CON and DSS rats, respectively. CL_R' of tofacitinib was considerably higher than CL_{CR} in CON rats (i.e., 2.49 mL/min/kg, Fig. 2), indicating that tofacitinib was actively secreted in the kidney as reported earlier (Lee and Kim, 2019). However, CL_R' of tofacitinib was lower than CL_{CR} in DSS rats (2.68 mL/min/kg, Fig. 2). This could be due to the significantly greater AUC due to the slower metabolism of tofacitinib in DSS rats, since the $Ae_{0\text{-}24\ h}$, CL_{CR}, and kidney histology in DSS rats were not significantly different from CON rats, indicating that kidney function was stable in both CON and DSS rats.

After the oral administration of tofacitinib to DSS rats, the AUC was also significantly greater than observed in CON rats, presumably due to a decrease in its metabolism in the intestine. Based on the *in vitro* intestinal metabolism of tofacitinib, its K_m values were comparable between CON and DSS rats, but V_{max} values were considerably slower in DSS rats, resulting in a slower CL_{int} in DSS rats than in CON rats (Fig. 6B). The slower intestinal CL_{int} in DSS rats was demonstrated by the decreased expression of CYP3A1/2 and CYP2C11 by 99.3% and 78.5%, respectively, in the intestine of DSS rats. The decreased expression of intestinal CYP3A1/2 and CYP2C11 was also due to a decrease in the expression of PXR and CAR in the intestine of DSS rats (Fig. 7B). The second peak in Fig. 4B was due to the individual difference in plasma concentration of DSS rats. One of DSS rats showed a very slow absorption and C_{max} of tofacitinib was very high at 180 min (2.22 μg/mL), which resulted in the second peak at 180 min in DSS rats (Fig. 4B). In addition, the protein level of P-gp was significantly decreased in the intestine of a DSS rat model (Yang *et al*., 2021), resulting in the improved absorption of tofacitinib, a substrate of P-gp (Hussar, 2014). Furthermore, gut microbiota is one of the reasons for the decrease in intestinal CYP3A and P-gp levels (Gao *et al*., 2017). Therefore, after the oral administration of tofacitinib to DSS rats, the greater AUC of tofacitinib was due to the increased absorption of tofacitinib due to decreased P-gp levels and slower metabolism of tofacitinib owing to decreased expression of CYP3A1/2 and CYP2C11. Increased membrane permeability may also contribute to the greater AUC of a drug in DSS rats. Dysfunction of the epithelial paracellular barrier and increase in mucosal permeability in the small intestine and colon contribute to increased absorption and result in significantly greater AUC of 6-carboxyfluorescein (Kumagai *et al*., 2020) and phenytoin (Kusunoki *et al*., 2017) in the DSS rat model.

Although the T/P ratios of tofacitinib were not significantly different between CON and DSS rats, the relatively lower T/P ratios in DSS rats were reflected in the lower V_{ss}, which was reduced by 43.2% in DSS rats. The decrease in V_{ss} appeared to be independent of plasma protein binding, which was comparable between the two groups (Fig. 2). Therefore, the significant increase in the plasma concentration of tofacitinib in DSS rats was due to the decrease in metabolism of tofacitinib, resulting in a lower V_{ss} and T/P ratio in DSS rats. Similar results have been reported for drugs such as oltipraz in a rat model of liver cirrhosis induced by *N*-dimethylnitrosamine (Ahn *et al*., 2009) and metformin in an acute renal failure rat model induced by gentamicin (Lee *et al*., 2013).

In summary, our pharmacokinetic results of tofacitinib showed that the AUC of tofacitinib increased significantly in DSS rats compared with CON rats, following the intravenous administration of tofacitinib, because of the slower CL_{int} in the liver owing to the decrease in the hepatic protein levels of CYP3A1/2 and CYP2C11. Similarly, after the oral administration of tofacitinib to DSS rats, the AUC was also significantly greater than that of CON rats due to slower intestinal CL_{int} owing to a decrease in the intestinal protein levels of CYP3A1/2 and CYP2C11. Decreased expression of P-gp also affected the greater AUC of tofacitinib in DSS rats. The pharmacokinetic changes of tofacitinib in DSS rats will provide useful information for deciding its clinical usage for patients with ulcerative colitis and will aid in the adjustment of tofacitinib dosage for these patients.

CONFLICT OF INTEREST

The authors declare that there are no competing financial interests.

ACKNOWLEDGMENTS

This work was supported by Basic Science Research Program (NRF-2021R1A2C1011142) through the National Research Foundation of Korea grant funded by the Ministry of Science and ICT, Republic of Korea.

REFERENCES

Ahn, C. Y., Bae, S. K., Bae, S. H., Kim, T., Jung, Y. S., Kim, Y. C., Lee, M. G. and Shin, W. G. (2009) Pharmacokinetics of oltipraz in diabetic rats with liver cirrhosis. *Br. J. Pharmacol.* **156**, 1019-1028.

Bae, S. H., Chang, S. Y. and Kim, S. H. (2020) Slower elimination of tofacitinib in acute renal failure rat models: contribution of hepatic metabolism and renal excretion. *Pharmaceutics* **12**, 714.

Baumgart, D. C. and Carding, S. R. (2007) Inflammatory bowel disease: cause and immunobiology. *Lancet* **369**, 1627-1640.

Bergan, T., Bjerke, P. E. and Fausa, O. (1981) Pharmacokinetics of metronidazole in patients with enteric disease compared to normal volunteers. *Chemotherapy* **27**, 233-238.

Cada, D. J., Demaris, K., Levien, T. L. and Baker, D. E. (2013) Tofacitinib. *Hosp. Pharm.* **48**, 413-424.

Changelian, P. S., Moshinsky, D., Kuhn, C. F., Flanagan, M. E., Munchhof, M. J., Harris, T. M., Whipple, D. A., Doty, J. L., Sun, J., Kent, C. R., Magnuson, K. S., Perregaux, D. G., Sawyer, P. S. and Kudlacz, E. M. (2008) The specificity of JAK3 kinase inhibitors. *Blood* **111**, 2155-2157.

Chen, C., Shah, Y. M., Morimura, K., Krausz, K. W., Miyazaki, M., Richardson, T. A., Morgan, E. T., Ntambi, J. M., Idle, J. R. and Gonzalez, F. J. (2008) Metabolomics reveals that hepatic stearoyl-CoA desaturase 1 downregulation exacerbates inflammation and acute colitis. *Cell Metab.* **7**, 135-147.

Chiou, W. L. (1978) Critical evaluation of the potential error in pharmacokinetic studies of using the linear trapezoidal rule method for the calculation of the area under the plasma level--time curve. *J. Pharmacokinet. Biopharm.* **6**, 539-546.

Claxton, L., Taylor, M., Soonasra, A., Bourret, J. A. and Gerber, R. A. (2018) An economic evaluation of tofacitinib treatment in rheumatoid arthritis after methotrexate or after 1 or 2 TNF inhibitors from a U.S. payer perspective. *J. Manag. Care Spec. Pharm.* **24**, 1010-1017.

Daujat-Chavanieu, M. and Gerbal-Chaloin, S. (2020) Regulation of CAR and PXR expression in health and disease. *Cells* **9**, 2395.

Dowty, M. E., Lin, J., Ryder, T. F., Wang, W., Walker, G. S., Vaz, A., Chan, G. L., Krishnaswami, S. and Prakash, C. (2014) The pharmacokinetics, metabolism and clearance mechanisms of tofacitinib, a Janus kinase inhibitor, in humans. *Drug Metab. Dispos.* **42**, 759-773.

Duggleby, R. G. (1995) Analysis of enzyme progress curves by nonlinear regression. *Methods Enzymol.* **249**, 61-90.

Fan, X., Ding, X. and Zhang, Q. Y. (2020) Hepatic and intestinal biotransformation gene expression and drug disposition in a dextran sulfate sodium-induced colitis mouse model. *Acta Pharm. Sin. B.* **10**, 123-135.

Flanagan, M. E., Blumenkopf, T. A., Brissette, W. H., Brown, M. F., Casavant, J. M., Shang-Poa, C., Doty, J. L., Elliott, E. A., Fisher, M. B., Hines, M., Kent, C., Kudlacz, E. M., Lillie, B. M., Magnuson, K. S., McCurdy, S. P., Munchhof, M. J., Perry, B. D., Sawyer, P. S., Strelevitz, T. J., Subramanyam, C., Sun, J., Whipple, D. A. and Changelian, P. S. (2010) Discovery of CP-690,550: a potent and selective Janus kinase (JAK) inhibitor for the treatment of autoimmune diseases and organ transplant rejection. *J. Med. Chem.* **53**, 8468-8484.

Fukuda, T., Naganuma, M. and Kanai, T. (2019) Current new challenges in the management of ulcerative colitis. *Intest. Res.* **17**, 36-44.

Gao, X. J., Li, T., Wei, B., Yan, Z. X. and Yan, R. (2017) Regulatory mechanisms of gut microbiota on intestinal CYP3A and P-glycoprotein in rats with dextran sulfate sodium-induced colitis. *Yao Xue Xue Bao* **52**, 34-43.

Gibaldi, M. and Perrier, D. (1982) Pharmacokinetics, 2nd ed. Marcel-Dekker, New York.

Gwak, E. H., Yoo, H. Y. and Kim, S. H. (2020) Effects of diabetes mellitus on the disposition of tofacitinib, a Janus kinase inhibitor, in rats. *Biomol. Ther.* (*Seoul*) **28**, 361-369.

Hu, N., Ling, J., Dong, L., Jiang, Y., Zhou, Q. and Zou, S. (2020) Pharmacokinetics of omeprazole in rats with dextran sulfate sodium-induced ulcerative colitis. *Drug Metab. Pharmacokinet.* **35**, 297-303.

Hussar, D. A. (2014) 2013 new drug update: what do new approvals hold for the elderly? *Consult. Pharm.* **29**, 224-238.

Kim, J. E., Park, M. Y. and Kim, S. H. (2020) Simple determination and quantification of tofacitinib, a JAK inhibitor, in rat plasma, urine and tissue homogenates by HPLC and its application to a pharmacokinetic study. *J. Pharm. Investig.* **50**, 603-612.

Kim, S. H., Lee, J. S. and Lee, M. G. (1999) Stability, blood partition and plasma protein binding of ipriflavone, an isoflavone derivative. *Biopharm. Drug Dispos.* **20**, 355-360.

Kumagai, M., Ishii, M., Morimoto, K. and Tomita, M. (2020) Increased membrane permeation and blood concentration of 6-carboxyfluorescein associated with dysfunction of paracellular route barrier in the small intestine of ulcerative colitis model rats. *Biopharm. Drug Dispos.* **41**, 91-100.

Kusunoki, Y., Kido, Y., Naito, Y., Kon, R., Mizukami, N., Kaneko, M., Wakui, N., Machida, Y. and Ikarashi, N. (2017) Changes in the pharmacokinetics of phenytoin in dextran sulfate sodium-induced ulcerative colitis in mice. *Int. J. Toxicol.* **36**, 485-491.

Kusunoki, Y., Ikarashi, N., Hayakawa, Y., Ishii, M., Kon, R., Ochiai, W., Machida,Y. and Sugiyama, K. (2014) Hepatic early inflammation induces downregulation of hepatic cytochrome P450 expression and metabolic activity in the dextran sulfate sodium-induced murine colitis. *Eur. J. Pharm. Sci.* **54**, 17-27.

Latteri, M., Angeloni, G., Silveri, N. G., Manna, R., Gasbarrini, G. and Navarra, P. (2001) Pharmacokinetics of cyclosporin microemulsion in patients with inflammatory bowel disease. *Clin. Pharmacokinet.* **40**, 473-483.

Lee, J. S. and Kim, S. H. (2019) Dose-dependent pharmacokinetics of tofacitinib in rats: Influence of hepatic and intestinal first-pass metabolism. *Pharmaceutics* **11**, 318.

Lee, Y. K., Chin, Y. W. and Choi, Y. H. (2013) Effects of Korean red ginseng extract on acute renal failure induced by gentamicin and pharmacokinetic changes by metformin in rats. *Food Chem. Toxicol.* **59**, 153-159.

Liu, Y. F., Niu, G. C., Li, C. Y., Guo, J. B., Song, J., Li, H. and Zhang, X. L. (2021) Mechanism of ulcerative colitis-aggravated liver fibrosis: the activation of hepatic stellate cells and TLR4 signaling through gut-liver axis. *Front. Physiol.* **12**, 695019.

Masubuchi, Y. and Horie, T. (2004) Endotoxin-mediated disturbance of hepatic cytochrome P450 function and development of endotoxin tolerance in the rat model of dextran sulfate sodium-induced experimental colitis. *Drug Metab. Dispos.* **32**, 437-441.

Mitruka, B. M. and Rawnsley, H. M. (1981) Clinical biomedical and hematological reference values in normal experimental animals and normal humans, 2nd ed. Masson Publishing, USA Inc., New York.

Mori, M., Stokes, K. Y., Vowinkel, T., Watanabe, N., Elrod, J. W., Harris, N. R., Lefer, D. J., Hibi, T. and Granger, D. N. (2005) Colonic blood flow responses in experimental colitis: time course and underlying mechanisms. *Am. J. Physiol. Gastrointest. Liver Physiol.* **289**, G1024-G1029.

Okayasu, I., Hatakeyama, S., Yamada, M., Ohkusa, T., Inagaki, Y. and Nakaya, R. (1990) A novel method in the induction of reliable experimental acute and chronic ulcerative colitis in mice. *Gastroenterology* **98**, 694-702.

Ordas, I., Eckmann, L., Talamini, M., Baumgart, D. C. and Sandborn W. J. (2012) Ulcerative colitis. *Lancet* **380**, 1606-1619.

Park, H. J., Bae, S. H. and Kim, S. H. (2021) Dose-independent phar-

macokinetics of loganin in rats: effect of intestinal first-pass metabolism on bioavailability. *J. Pharm. Investig.* **51**, 767-776.

Pastor Rojo, O., López San Román, A., Albéniz Arbizu, E., de la Hera Martínez, A., Ripoll Sevillano, E. and Albillos Martínez, A. (2007) Serum lipopolysaccharide-binding protein in endotoxemic patients with inflammatory bowel disease. *Inflamm. Bowel Dis.* **13**, 269-277.

Sandborn, W. J., Peyrin-Biroulet, L., Sharara, A. I., Su, C., Modesto, I., Mundayat, R., Gunay, L. M., Salese, L. and Sands, B. E. (2022) Efficacy and safety of tofacitinib in ulcerative colitis based on prior tumor necrosis factor inhibitor failure status. *Clin. Gastroenterol. Hepatol.* **20**, 591-601.

Sartor, R. B. (2008) Microbial influences in inflammatory bowel diseases. *Gastroenterology* **134**, 577-594.

Scott, L. J. (2013) Tofacitinib: a review of its use in adult patients with rheumatoid arthritis. *Drugs* **73**, 857-874.

Shin, W. G., Lee, M. G., Lee, M. H. and Kim, N. D. (1991) Factors influencing the protein binding of vancomycin. *Biopharm. Drug Dispos.* **12**, 637-646.

Solomon, L., Mansor, S., Mallon, P., Donnelly, E., Hoper, M., Loughrey, M., Kirk, S. and Gardiner, K. (2010) The dextran sulphate sodium (DSS) model of colitis: an overview. *Comp. Clin. Pathol.* **19**, 235-239.

Svein, Ø. and Theodor, W. G. (1982) Comparison of equilibrium time in dialysis experiments using spiked plasma or spiked buffer. *J. Pharm. Sci.* **71**, 127-128.

Taurog, J. D., Richardson, J. A., Croft, J. T., Simmons, W. A., Zhou, M., Fernández-Sueiro, J. L., Balish, E. and Hammer, R. E. (1994) The germfree state prevents development of gut and joint inflammatory disease in HLA-B27 transgenic rats. *J. Exp. Med.* **180**, 2359-2364.

Wada, T., Gao, J. and Xie, W. (2009) PXR and CAR in energy metabolism. *Trends Endocrinol. Metab.* **20**, 273-279.

Yang, Y., Hu, N., Gao, X. J., Li, T., Yan, Z. X., Wang, P. P., Wei, B., Li, S., Zhang, Z. J., Li, S. L. and Yan, R. (2021) Dextran sulfate sodium-induced colitis and ginseng intervention altered oral pharmacokinetics of cyclosporine A in rats. *J. Ethnopharmacol.* **265**, 113251.